We are IntechOpen,
the world's leading publisher of
Open Access books
Built by scientists, for scientists

6,900
Open access books available

185,000
International authors and editors

200M
Downloads

154
Countries delivered to

Our authors are among the

TOP 1%
most cited scientists

12.2%
Contributors from top 500 universities

WEB OF SCIENCE™

Selection of our books indexed in the Book Citation Index
in Web of Science™ Core Collection (BKCI)

Interested in publishing with us?
Contact book.department@intechopen.com

Numbers displayed above are based on latest data collected.
For more information visit www.intechopen.com

Use of Magnetic Induction Spectroscopy in the Characterization of the Impedance of the Material with Biological Characteristics
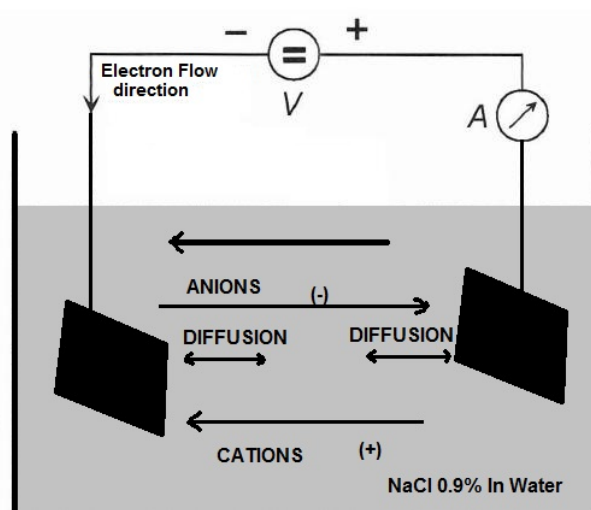
Jesús Rodarte Dávila, Jenaro C. Paz Gutierrez and Ricardo Perez Blanco

1. Introduction

The basic electrolytic experiment consists of a homogeneous[1] electrolytic solution with two identical electrodes (Fig 1). We know that a homogeneous solution hasn't boundaries or membranes, except the electrodes and the solution receipt.


Figure 1. The basic electrolytic experiment

Electrolyte solution selected as the most important of the human body: NaCl aqueous solution with a concentration of 0.9% by weight [i].

---

[1] If NaCl is dissolved in water then NaCl is the solute (and the electrolyte), and water is the solvent, together form the solution

In a homogeneous conductive material the impedance (Z) is proportional to its length and inversely proportional to its cross sectional area (A) (Fig. 2).
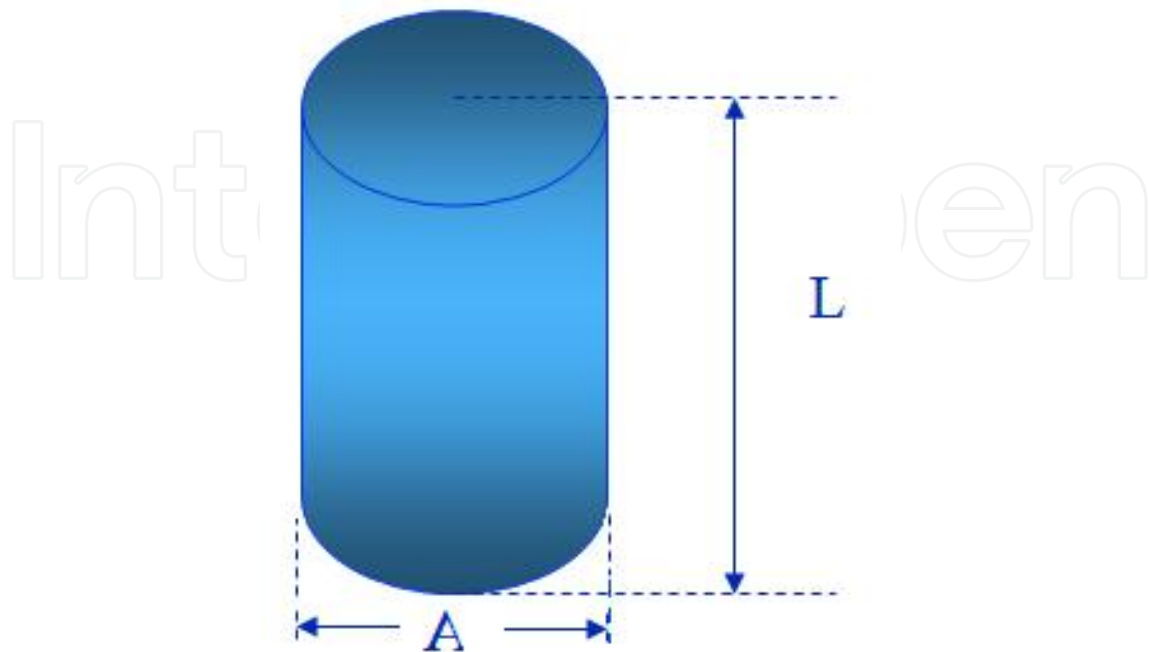
Figure 2. The impedance (Z) of homogeneous conductive material is directly proportional to its length and resistivity and inversely with its area

$$Z = \varrho L / A = \varrho L^2 / V \tag{1}$$

According with the Figure 2 Z=impedance, L=length, A=area, V=volume ϱ=resistivity=1/σ (conductivity). An empirical relationship can be established between the ratio (L^2 / V) and the impedance of the saline solution which contains electrolytes that conduct electricity through the sample. Therefore impedance (Z) = $\rho L / A = \rho L^2 / V$.

Hoffer et al. [2] and Nyboer [3] were the first to introduce the technique of four surface electrodes Bio-impedance analysis.

A disadvantage presented by this technique is the use of a high current (800 mA) and a high voltage to decrease the volatility of injected current associated with skin impedance (10 000 Ω/cm^2)[4]

Harris et al.[5], (1987) uses a four terminals device to measure impedance for the purpose of eliminating the effect of electrodes in an aqueous medium.

Asami et al.[6] , (1999) used a pair of coils submerged for monitoring the current induced in the coil pair, which he called electrode-less method, however still requires physical connections between the coils and electronic instruments.

To measure the complex spectrum of the permittivity of a biological culture solution Ong et al.[7], uses a remote sensor resonant circuit, to obtain the impedance of the environment by observing the resonant frequency and the frequency of zero reactance.

In another case for monitoring the fermentation process Hofmann et al.[8], Use a sensor based on a transceiver, as a way of overcoming the effect of having two metal electrodes to measure the impedance of the culture broth in a fermentation process, as in such processes the behavior of living cells is as small capacitors, then measure the impedance represented by these small capacitors correlates with the number and size of living cells in the system (Hofmann et al., 2005).

2. Magnetic induction spectroscopy

"The Magnetic Induction Spectroscopy (MIS) aim is the non-contact measurement of passive electrical properties (PEP) σ, ε and μ of biological tissues via magnetic fields at various frequencies.[9]"

The basic requirements of this method are:

a. Creating a varying in time magnetic field, from an exciting coil to induce the field to the object under study.
b. Obtaining information generated from the disturbance or "reaction" of coils-environment system through the Receiver / Sensor coil.
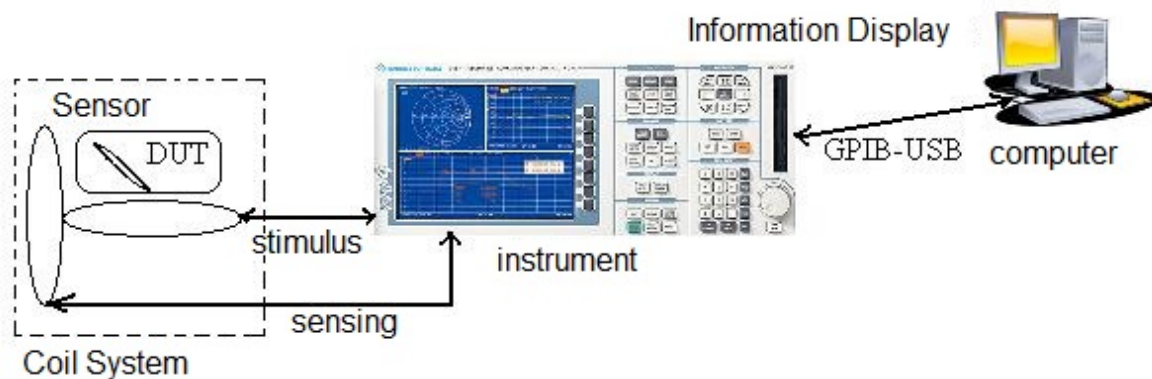

Figure 3. Measurement System: composed of a coil arrangement, network analyzer, and a pc
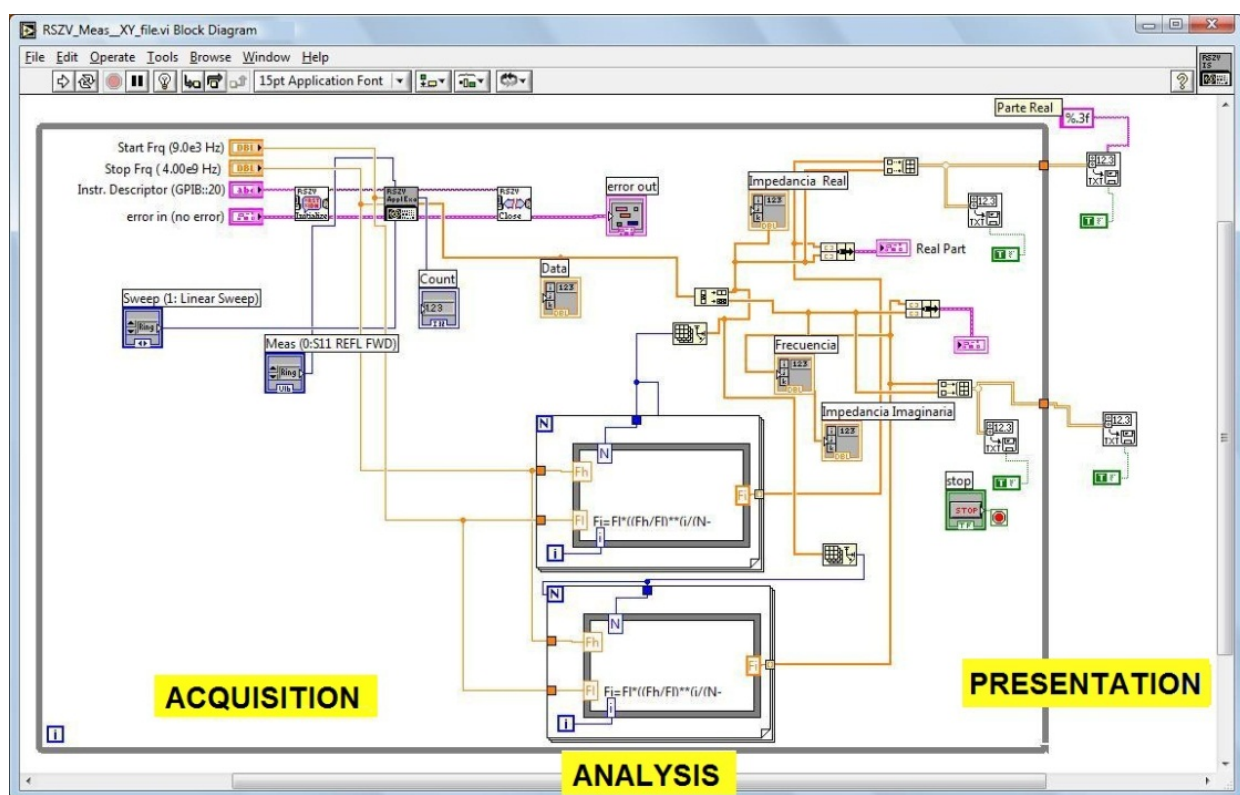
3. Measurement system

Following the protocol of the method used in Figure 3 we present our system Equipment-Interface into three sections:

a. Computer: Using the platform that provides National Instrument [10] - LabView V8.6, displays and processes the information obtained from the coil system from the Instrument.
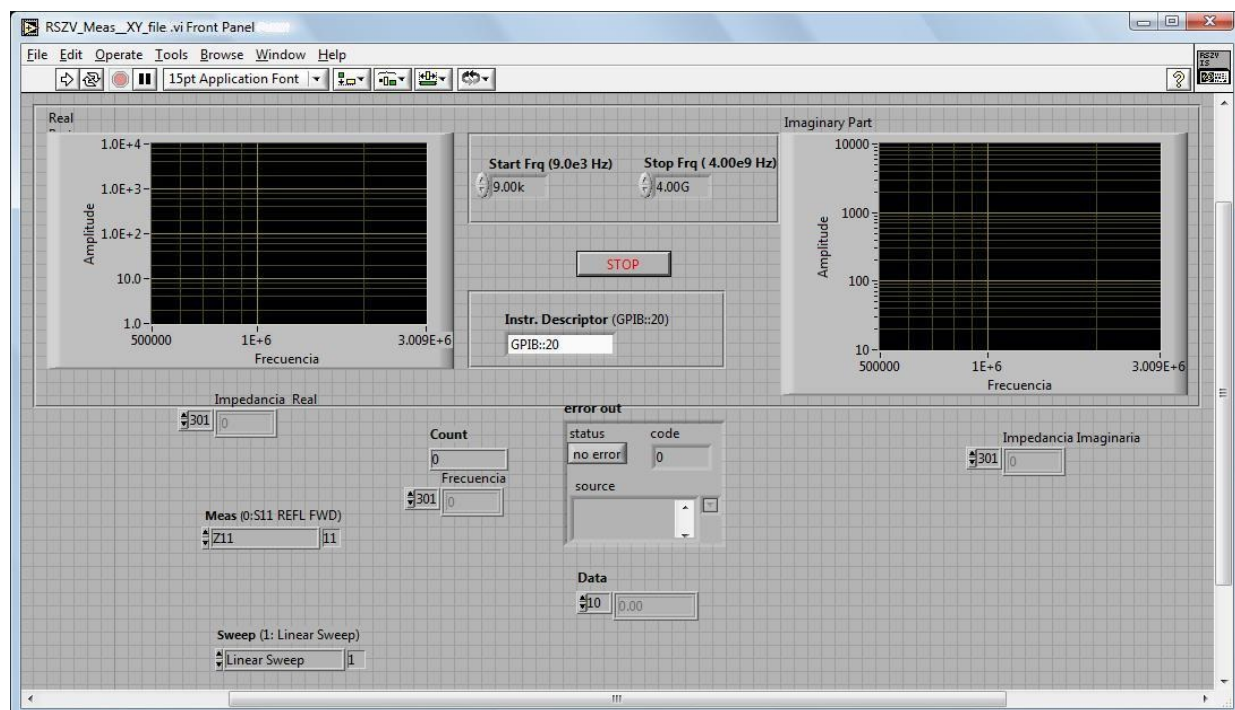
(a)

(b)

Figure 4. Virtual Instruments LabVIEW (National Instrument VI), a) Front panel (user), b) Block diagram panel (interconnections), uses them to automate the acquisition and management of information.

b. Instrument: Commercial Equipment, RS ZV Vector Network Analyzer [11] "Rohde &
    Schwartz" which performs the frequency sweep from 100 kHz to 4 MHz range,
    applying it to the exciting coil, the same equipment then captures the data or
    information from the receiver coil and sends to the computer via General-Purpose
    Interface Bus Universal Serial Bus or GPIB-USB.
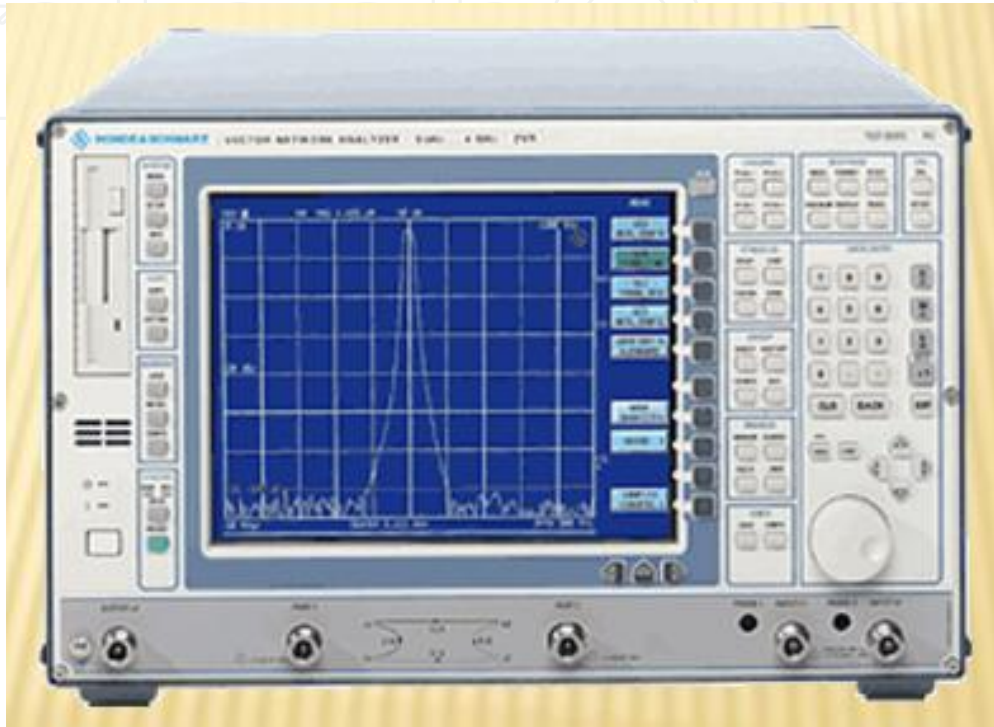
Figure 5. Network Analyzer "Rohde & Schwartz", as a frequency sweep source

c. Coil System: Fig. 6 show this system, consisting of three coils, an exciter, a receiver
    completely perpendicular to the exciting, adjusting it to the mutual inductance between
    two coils is minimal, and a third coil to function as "mirror-sensor" of the magnetic field
   generated by the exciting coil.
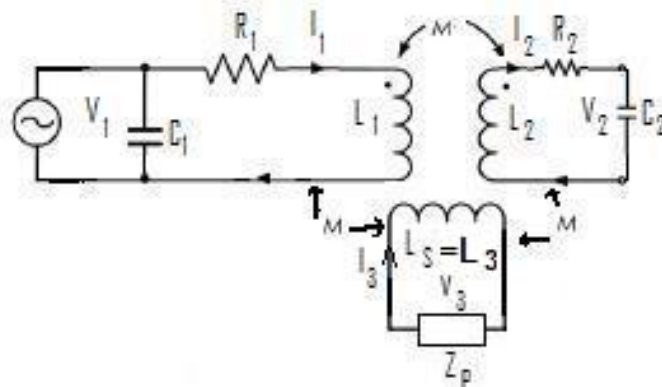
Figure 6. Representative schematic of the three coil arrangement

3.1. Drive coil L1

For generating a spectral magnetic field a flat coil was used as a transmitting antenna built on a phenol board as printed circuit with the following characteristics:

- Spiral coil [12] internal diameter of 2 cm and an outer diameter of 9.5 cm with 20 turns, with cooper tracks width of 500 μm , and an equal distance between them, see Figure 7
- 24 μH Inductance measured experimentally in a frequency range of 100 KHz to 5 MHz
- Shielding is used to minimize capacitive coupling at the top and bottom of the exciting coil, forming a sandwich, this shielding was "grounded".
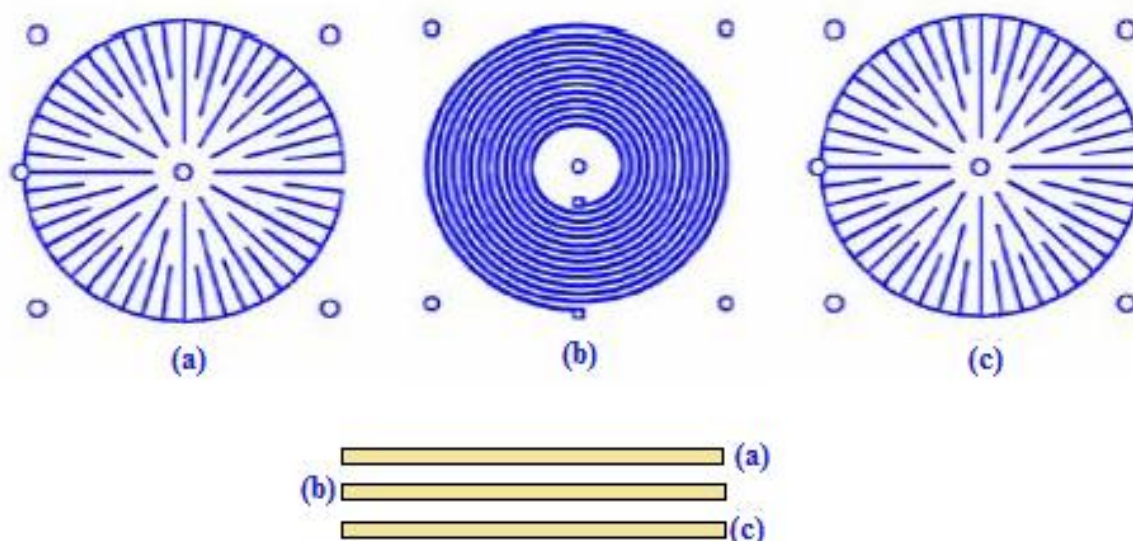

Figure 7. Coil and Shielding employee

The Network Analyzer employee served as a source of power in a frequency range of 100 KHz to 5 MHz applied. The combination coil and capacitance of the cables, that although were coaxial cables it presented a resonance frequency of 4.612 MHz This initial structure was proceeded with a series of measurements with actual physical capacitors with a dual role, first see the system answer at different values, and the second as reference calibration [13].

3.2. Receiver coil L2

For reception of the spectrum magnetic field, also use a flat coil as the receiving antenna, built on a phenol board as printed circuit with the following characteristics almost as similar to the transmitting antenna:

- Spiral coil internal diameter of 2 cm and an outer diameter of 9.5 cm with 20 turns, with cooper tracks width of 500 μm, and an equal distance between them, see Figure 8
- 24μH Inductance measured experimentally in a frequency range of 100 KHz to 5 MHz
- Shielding is used to minimize capacitive coupling in the bottom of the receiving coil, this shield was "grounded".
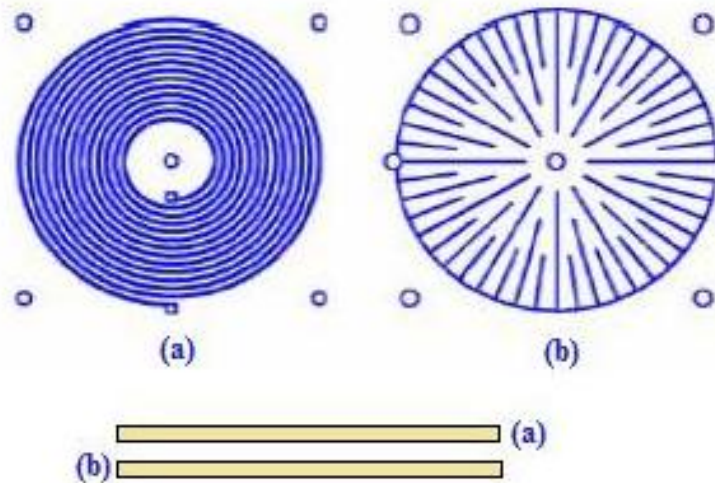
Figure 8. Coil and shield used

• In addition to the above conditions and in order to minimize inductive coupling both coils are placed in perpendicular way see Figure 9, so that the only magnetic field received were the projected by the coil sensor.
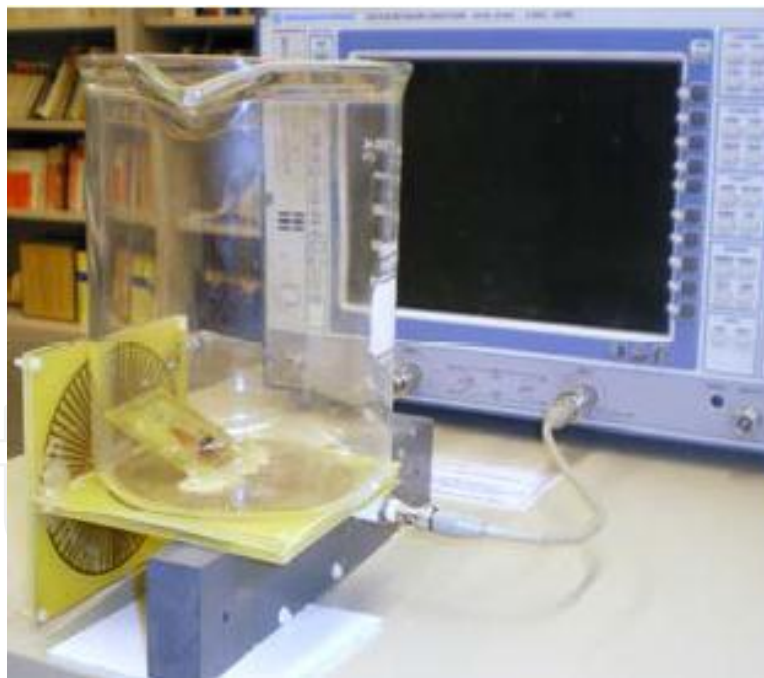
Figure 9. Mechanical available of the coils to minimize Inductive coupling between transmitter coil and receiver coils

Network Analyzer employee close the system, as seen in Figure 9, the application is through the coil L1, placed horizontally, which serves as basis for the deposition of both the saline and the samples biological tissue. Receiving and monitoring of the signal through the coil L2, vertically positioned and perpendicular to L1
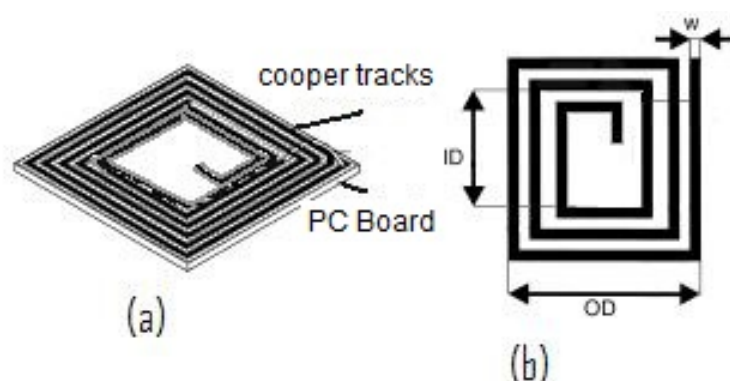
3.3. Mirror-sensor coil

As a passive coil mirror-sensor used a flat square coil of about 7.92 µH, see Figure 10, with a measured value of 9.716 µH, at a frequency applied of 1 MHz, Coil with a capacitor of 330 nF added to make a 1 MHz resonant circuit, finally resulting a resonant frequency of 1.14 MHz, like the previous coils was constructed on phenol board as a printed circuit having the following characteristics:

- The inductance L, was determined by experimental measurements, confirming the calculations used in the approximation developed by Ong et al[14].

$$L = 1.39 * 10^{-6}(OD + ID) * N_L^{\frac{5}{3}} * log(4 * \frac{OD+IDD}{OD-ID}) \qquad (2)$$

Figure 10. Layout of the Mirror-Sensor coil with interdigital capacitor (not shown)

- Square spiral coil internal diameter of 3.6 cm and an outer diameter of 4.7 cm with 10 turns, according to the expression [1] L = 7.92 µH
- To minimize resistive-capacitive effect between turns, when immersed in saline was used an insulating paint.

4. Characterization of the system

The technique of network development has in its whole with the element to explore interesting properties, which generates all possible parameters of the immittance associated with the two-port network, Figure 11.
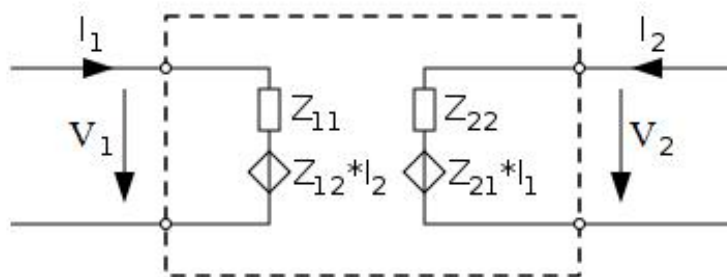
Figure 11. Electronic models of the transmitter coil and receiver coil

The formulation of network equations obtained by choosing voltages across the capacitors which are not physically in our arrangement, but it is necessary to include consideration coaxial cables within the coil system, which by their physical characteristics have a value of capacitance and current flows through the antenna-coils (inductors) as variables used in the description of the network, produces many equations as reactive elements present in a given network.

VI relations of our model, without loss, respecting the conventions of voltage and current shown in Figure 11, are[15]:

$$V_1 = Z_{11} * I_1 + Z_{12} * I_2 \tag{3}$$

$$V_2 = Z_{21} * I_1 + Z_{22} * I_2 \tag{4}$$

Since the primary reactive elements of this network are the inductors $Z_{11} = j\omega L_1$ y $Z_{12} = j\omega M$; $Z_{22} = j\omega L_2$ y $Z_{21} = {}_j\omega M$ and since there is an inductive link between the coils, equations [2] and [3] are reconsidered:

$$V_1 = j\omega L_1 * I_1 + j\omega M * I_2 \tag{5}$$

$$V_2 = j\omega M * I_1 + j\omega L_2 * I_2 \tag{6}$$

in equations [4] and [5], M is the mutual inductance (dimension H) between the coils L_1 and L_2, defined by $M = k * \sqrt{L_1 * L_2}$ where k (dimensionless number, ≤ 1) is the coupling factor between the inductors (inductive link ratio), controllable with the relative position between them.

The model presented in Figure 6 allows the development of matrix impedance parameters of a bi-port, as expressed in equations [3-6], and involves the mutual inductance of the coil system, then presents the mathematical analysis of the inductive link.

The design and structure of the coil system aims to make the inductive link between the coils L1 and L2 is minimized by establishing a physical way the perpendicularity between L1 and L2, seeking with this strategy to establish a relationship of mutual inductance increased by engaging in two-port network a third coil that provides a "mirror" effect, the Figure 12 shows a representation of the this inductive link.

The mutual inductance M_{12} of the inductor L_2 in relation to L_1, which (according to the reciprocity theorem) it was found experimentally equal to the mutual inductance M_{21} of the inductor L_1 in relation to L_2, theoretically defined as the coefficient of mutual magnetic flux $\Phi_{12} = \Phi_{21}$ which spans both coils due to the current flowing in each coil respectively.

$$M_{12} = \frac{\Phi_{12}}{I_1} \tag{7}$$

$$M_{21} = \frac{\Phi_{21}}{I_2} \tag{8}$$

"The Biot-Savart law, states that if a small length of conductor δl carrying a current i, then the magnetic field strength at a distance r and angle θ is

$$\delta H = \frac{i\delta l sin\theta}{4\pi r^2} \tag{9}$$
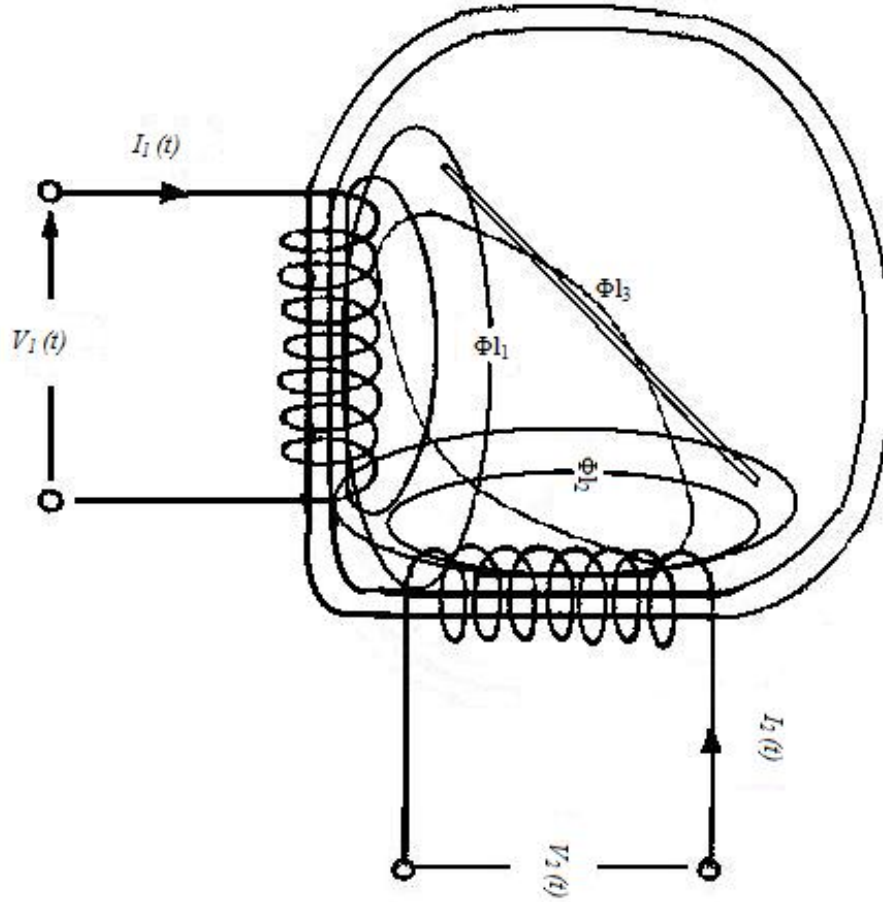
Figure 12. Approximate representation of variable in time magnetic induction in the coils system

(Sine θ merely states that if power is not in an optimal direction, then the field at that point decreases.) This is confirmed by Ampere's rule, $\int H dl = i$; The line integral of the magnetic field in a closed loop is equal to the electric current flow through the closed loop" [16]. In particular, the magnetic field strength H in a circular path of radius r around an electric current i in the center is

$$H \cdot 2\pi r = i, o\ B = \frac{\mu i}{2\pi r} \qquad (10)$$

Because L_1 and L_2 have very similar characteristics, and considering the expression [9] may approximate the magnetic field concentric loops through both coils (see Figure 8a), B_1 is the magnetic field of the first ring, the flow magnetic Φ_2 through second ring we can determine from B_1.

$$\Phi_2 = B_1 A_2 = \left(\frac{\mu_0 I_1}{2R_1}\right)\pi R_2^2 = \frac{\mu_0 \pi I_1 R_2^2}{2R_1} \qquad (11)$$

where μ_0 is the magnetic permeability of free space, R_1 and R_2 are the radii of the rings which form the coils.

The mutual inductance is then:

$$M = \frac{\Phi_2}{I_1} = \frac{\mu_0 \pi R_2^2}{2R_1} \qquad (12)$$

This expression shows that M depends only on geometric factors, R_1 and R_2, and is independent of the current in the coil. As regards the expression $M = k * \sqrt{L_1 * L_2}$ to obtain an approximation of mutual inductance between coils, since low values of coupling coefficients "k" with air-core coils are obtained usually in the order of 0.001 to 0.15 [17] experimentally is considered as the value of $k_1 = 0.00167$ (caused by a misalignment both angular and lateral between coils L_1 and L_2), and a value of $k_2 = k_3 = 0.465$ (caused by an angular misalignment between coils L_1, L_2 over L_3), so we get the following values:

$$M_{31} = M_{13} = 7.1\mu H$$

$$M_{23} = M_{32} = 7.1\mu H$$

$$M_{21} = M_{12} = 0.04 \ \mu H$$

By obtaining these values, we proceeded to simulate the circuit in PSpice [18], see Figure 13, to verify that they were not far from the actual physical model, which was obtained following graphs.
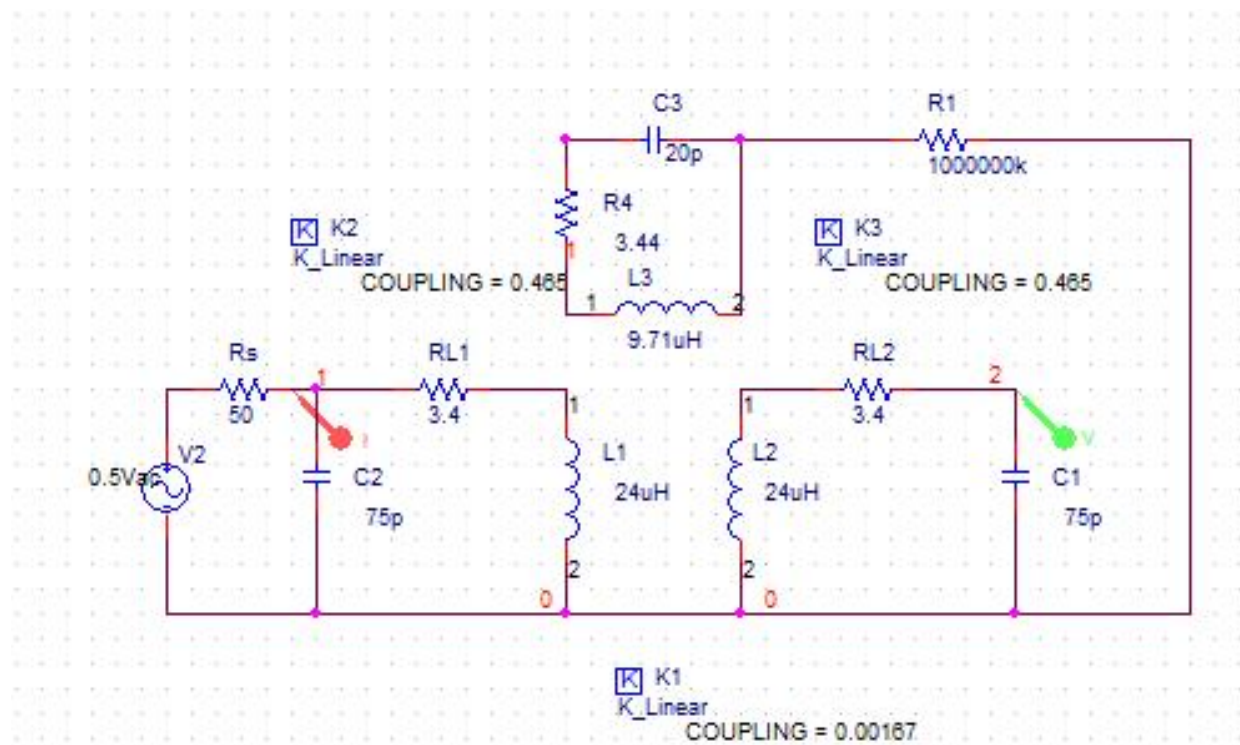
Figure 13. System coils with their respective coupling factors for achieving the simulation circuit had to be "grounded" L3 but with the highest permissible value, simulating a physical disconnection between the two coils.

In Figure 14 we can observe the system performance in terms of voltage induction refers to both L_2 and L_3.
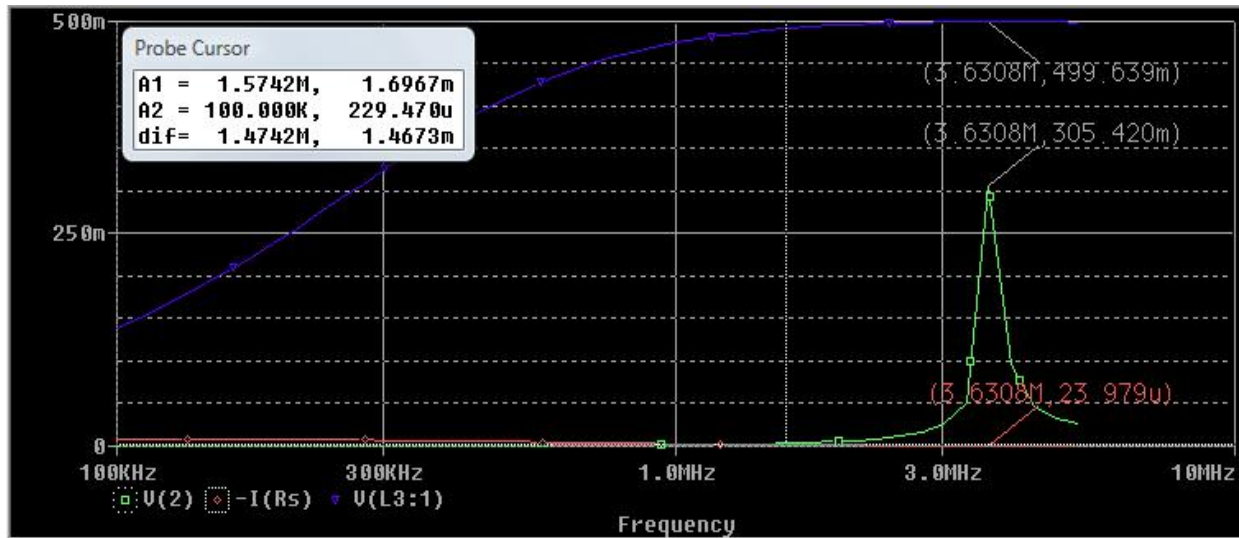
Figure 14. Response of the coil system to a frequency sweep from 100 kHz to 5 MHz, with estimated coupling factors.

The obtained simulation results permit the development equations which describe the model in Figure 6; these can be expressed in matrix form:

$$\begin{bmatrix} V_1 \\ V_2 \\ V_3 \end{bmatrix} = j\omega \begin{bmatrix} L_1 & M_{12} & M_{13} \\ M_{21} & L_2 & M_{23} \\ M_{31} & M_{32} & L_3 \end{bmatrix} \begin{bmatrix} i_1 \\ i_2 \\ i_3 \end{bmatrix} \tag{13}$$

Mij are mutual inductances, and the proportionality factors of the currents are the impedances so that the matrix can be rewritten in terms of the Z parameters.

$$\begin{bmatrix} V_1 \\ V_2 \\ V_3 \end{bmatrix} = j\omega \begin{bmatrix} Z_{11} & Z_{12} & Z_{13} \\ Z_{21} & Z_{22} & Z_{23} \\ Z_{31} & Z_{32} & Z_{33} \end{bmatrix} \begin{bmatrix} i_1 \\ i_2 \\ i_3 \end{bmatrix} \tag{14}$$

As experimentally determined that $Z_{12} = Z_{21}$ be as small as possible to perceive impedance changes as the sensor coil L_3, so we have:

$$Z_{12} = \frac{V_1}{i_2}|i_1 = 0; \; Z_{21} = \frac{V_2}{i_1}|i_2 = 0$$

$$\frac{V_3}{i_3} = Z_3 \tag{15}$$

If we consider the equations [14] and [15] in combination with the matrix [12], expressing V2 in terms of Z3, we have:

$$V_2 = j\omega M_{21} i_1 + j\omega M_{23} \frac{V_3}{Z_3} \tag{16}$$

5. Making a reference

Considering the previous development, and articles concerning the use of systems like ours (Ong. 2000, Hofmann 2005) is therefore important to have baseline measurements

of physical elements such as capacitors, to be served at one time as models of reference and calibration, was determined to carry out the completion of the procedure detailed below.

Figure [16] the electrical circuit presented is the model of a capacitive type humidity sensor [19], the behavior of this sensor is comparable to the behavior of L_3 so we can take the development of the equation for Z_P that would be the Z_3 response, which could take the complex impedance as:

$$Z_P = R_s + \frac{R_p}{1+j\omega R_P C} \tag{17}$$

Misevich et al refers to the resistance changes predominantly in the range of 10-100 MΩ in a circuit as shown in Figure [15], fall about 0.5 Ω in a very humid environmental, is not our case so is taken as a criterion for considering a single value of R_P of 100Ω, likewise considering the impedance presented by R_P, varying ω in the range of $12e^{+6}$ to $25e^{+6}$ rad / s the impedance C in parallel with R_P take R_P value in the range of C values from 10pF-100pF, and goes to take the R_s value in the range of C values from 1nF-100nF, see table 1, that added to the XL values presented by ω is negligible this value so we can reduce our equation to:

$$Z_P = \frac{R_P}{1+j\omega R_P C} \tag{18}$$
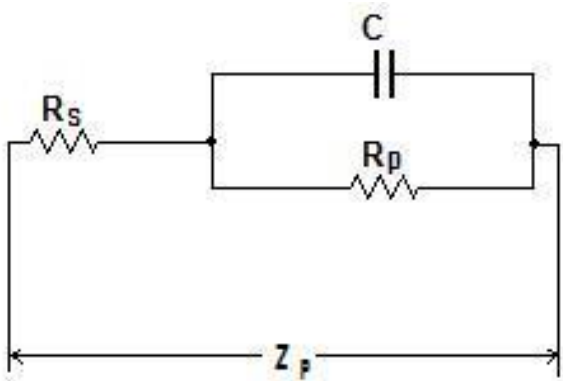
Figure 15. Misevich, K.W. shows the development of a capacitive humidity sensor element impedance equivalent to measuring the coil system, where R_s = 3.44Ω series resistance of the sensor, R_P = 100Ω, C multivalued see table 2

Val. Cap./Freq.	2.5MHz	3MHz	3.5MHz	4MHz
10pF	98.4Ω	98.1Ω	97.8Ω	97.5Ω
100pF	86.4Ω	84.1Ω	82Ω	80.0Ω
1nF	38.9Ω	34.6Ω	31.25Ω	28.5Ω
10nF	5.98Ω	5.04Ω	4.35Ω	3.82Ω
100nF	0.63Ω	0.53Ω	0.45Ω	0.4Ω

Table 1. Z_P = Z_3 values obtained by calculation.

$$Z_3 := \frac{R_3}{1+(j \cdot R_3 \cdot C_3)} = 97.459 - 17.73i \tag{19}$$

Expression [19] used for calculating the impedance of Table 1 using MathCad [20]; Therefore the values obtained with small capacitors values by calculating means as measured by the analyzer is in a range of 5% in 3.09 MHz, the resonance frequency, and not higher capacitor values that are very de-correlated, this is due to the length of the coaxial cables, overriding the capacitance introduced by these.

Val. Cap./Freq.	2.5MHz	3MHz	3.5MHz	4MHz
10pF	96.18Ω	102.7Ω	107.8Ω	112Ω
100pF	100.9Ω	107Ω	110.5Ω	112.6Ω
1nF	60.2Ω	41.4Ω	29.5Ω	24.5Ω
10nF	22.6Ω	29.6Ω	36.2Ω	42.7Ω
100nF	29.6Ω	35.7Ω	41.7Ω	47.63Ω

Table 2. Z_3 values obtained by direct measurement by network analyzer.

If we consider the matrix equation [12] and equation [18], V_3 can be expressed in terms of $Z_P = Z_3$, we have then:

$$V_3 = \frac{j\omega M_{23} i_2}{1 - \frac{j\omega L_S}{Z_3}} \tag{20}$$

Considering the matrix equation [12] and equation [19], we have V_1 expressed in terms of Z_3:

$$V_1 = j\omega M_{12} i_2 + j\omega M_{13} \left(\frac{j\omega M_{23} i_2}{Z_3 - j\omega L_S} \right) \tag{21}$$

If we consider the equation [14 and 20] we express Z_{12} as:

$$Z_{12} = j\omega M_{12} - \omega^2 \left(\frac{M_{23} M_{31}}{\sqrt{\left(\frac{1}{R_P}\right)^2 + (\omega C)^2} - j\omega L_S} \right) \tag{22}$$

Figure 16 shows the values obtained by performing calculations using equation [22] implemented in Mathcad, it is appreciated also that around the two resonance frequencies in the system the magnitude of Z_{12} is the same.
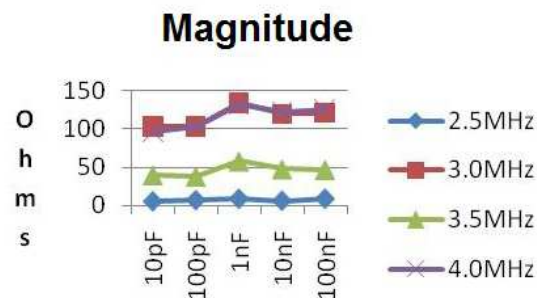
Figure 16. Comparison between Z_{12} Magnitude values of impedance calculation in Mathcad.

6. Validation and calibration

Figure 17a shows the graphical model used for our experiment, and Figure 17b refers as a practical way to the interface between the network analyzer and sensor description given above in a comprehensive manner.
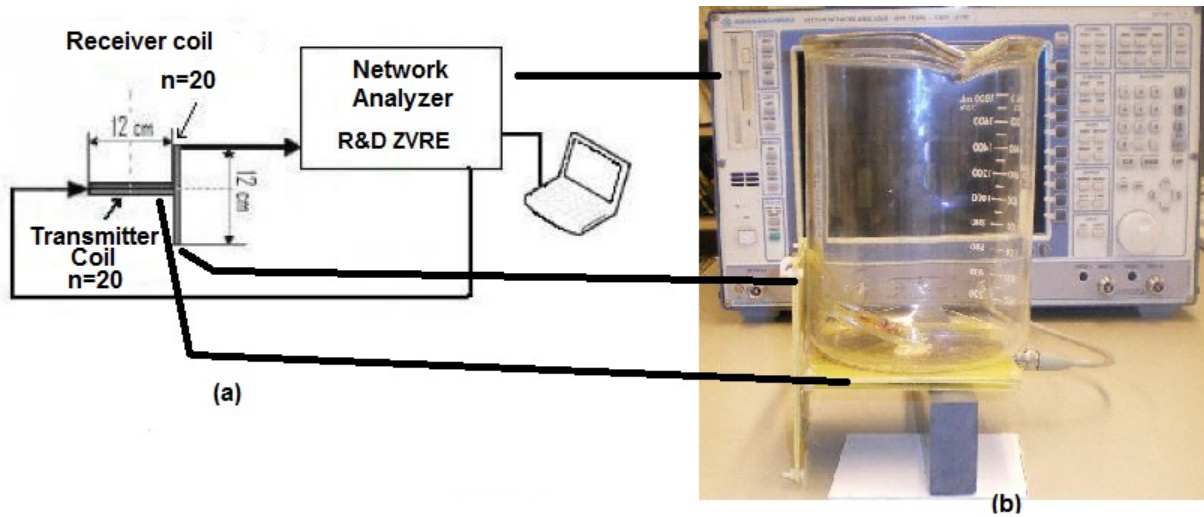
Figure 17. Magnetic Impedance Spectroscopy Method: a) block diagram, and b) practical implementation

Figure 18 a shows a block diagram of a three-port circuit, the voltages and currents are indicated, the upper terminal of the instance is positive with respect to the terminals of the bottom and the currents flowing inwards as indicated by KCL for each port, Figure 18b shows the block diagram of a real form.
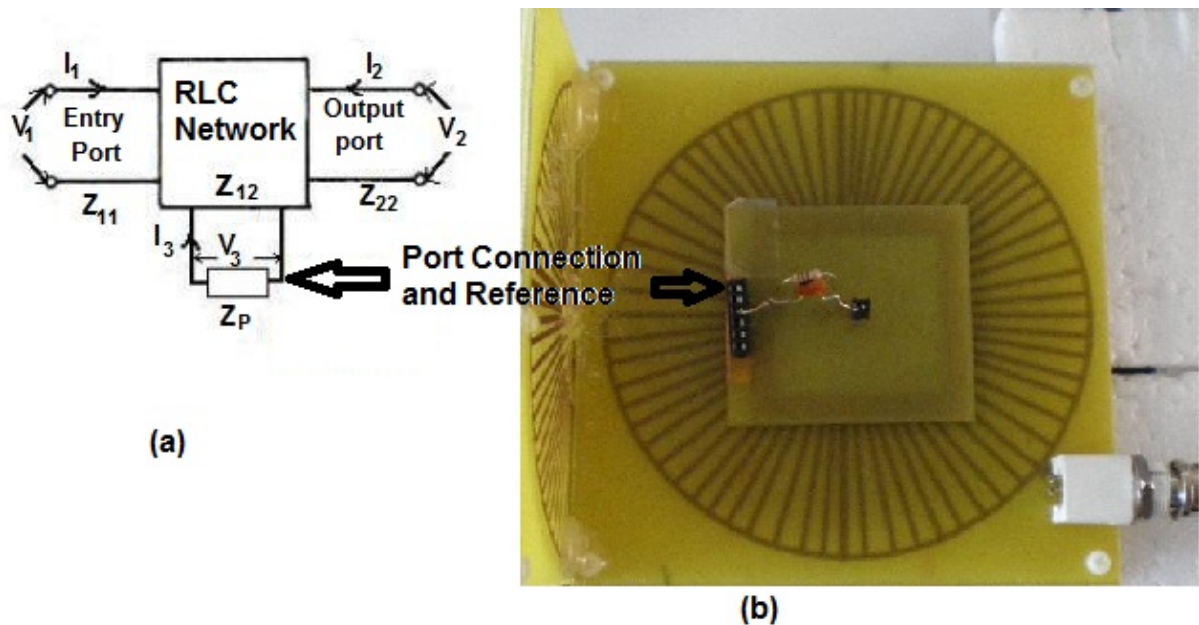
Figure 18. Three-port circuit in preparation for constant section cell measuring based on measurement of physical components.
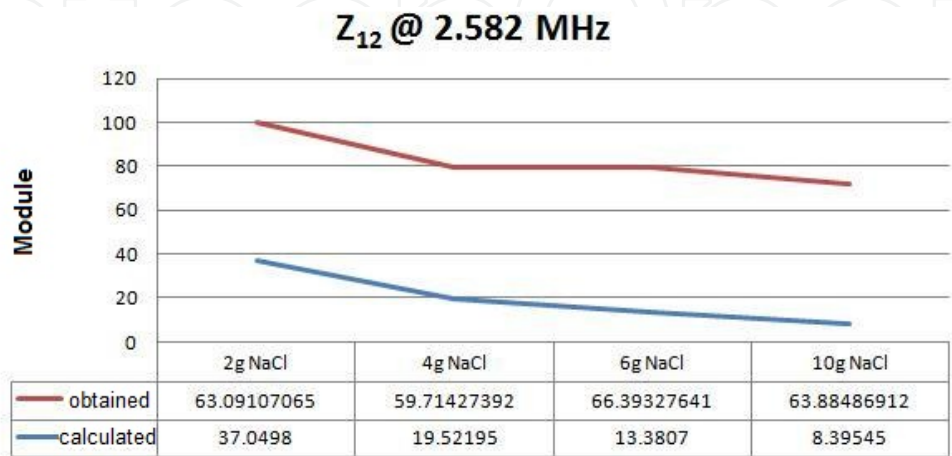
The values obtained for both measurement and calculation as shown in Table 2 allows us to make the cell preparation of constant section for measuring conductivity. For this preparation had to consider the mechanical error sources such as physical dimensions of the saline cell, the effects of temperature on the cell, and error handling and positioning of it. It also ponder the discrepancy between the measurements of a real physical element such as a capacitor in parallel with a resistor, and the resistivity and permittivity expected of an electrolytic cell, it was therefore necessary to have a truer reference of known salt solution to evaluate deviation of our measurements and bring the measuring physical model to a virtual model and simulate their behavior in this way to "induce" their performance, come to perform these measurements with electrodes.

In Figure 19 shows a sample obtained from a series of measurements made under the scheme of Figure 18, changing the values of the capacitances in parallel with resistors first small values, reaching values used to 1 kΩ .
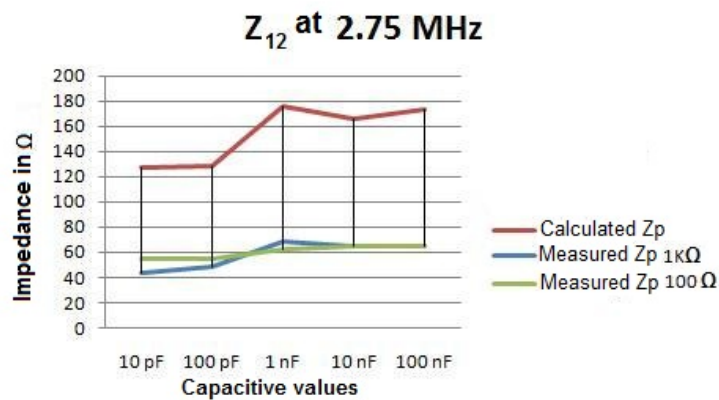

Figure 19. Comparisons between reference measurements with physical components and estimated values

Although performing multiple measurements and their subsequent acquisition of information due to the speed and flexibility of use of equipment to automate this process, include only the most representative of the behavior of a saline cell, as seen in Figure 20, with various degrees of salinity.

	2g NaCl	4g NaCl	6g NaCl	10g NaCl
obtained	63.09107065	59.71427392	66.39327641	63.88486912
calculated	37.0498	19.52195	13.3807	8.39545

Figure 20. Measurement of Z_{12} of four saline cells

Values obtained with the saline cell, Figure 20, as well as the physical components are between 4% and 8% above the Z12 average obtained from the saline cell, provides that comparatively physical model is closer to cell model representing a saline cell of Figure 21, which is formed by a resistance of 100 Ω in parallel with a capacitor of 1 nF, with a response very "right" to the resonant frequency of the coil system which is approximately 3 MHz
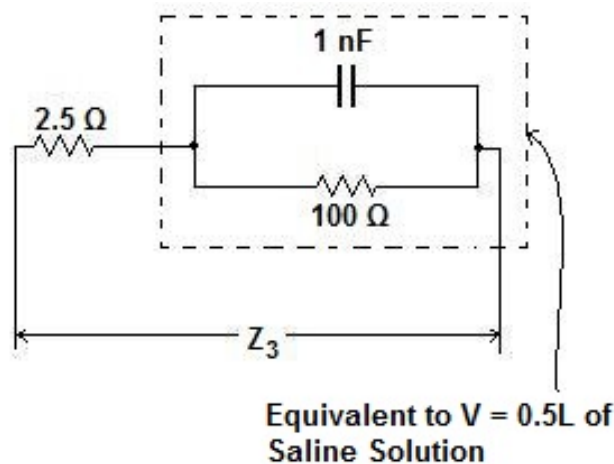
Figure 21. Physical model equivalents to a 500 mL saline cell at a frequency of ~ 3 MHz

The conductivity of a saline solution with 2 g of salt dissolved in 1L of deionized water having a conductivity measurement 5.8μS/cm, presents a σ = 3.9 mS / cm at 25 ° C and σ = 3.4 mS / cm at 20 ° C, this represents a 0.2% concentration and 0.034 M.

If we use this solution as the first reference electrolytic cell and according to equation [1], with an equal volume to 500 mL and a length of 85 mm, we calculate a 37.05Ω impedance (Z) , with these values and data from our physical model equivalent gives a σ = 2.29 mS / cm which leads us to obtain a correction term 3.9/2.29 = 1.7.

7. Measuring saline cell permittivity with mis

The resistivity of an aqueous sodium chloride dissolution (NaCl) [21] is obtained from considering the current density (J), determined this by the ions types (Na $^+$ and Cl $^-$ are the most abundant ions) of the solution, this is directly proportional to the factor "α" of dissociation of molecules, approximately equal to 1 if the electrolyte is strong, with a concentration "c "gram-equivalent, and a mobility" μ "of the ions, also the electric field" E "as shown in the following relationship: J = F α c μ E.

A solution consisting of 9 grams of sodium chloride dissolved in one liter of water in medicine[2] is called Normal Saline, since the concentration of 9 grams per liter divided by 58 grams per mole (approximate molecular weight of sodium chloride) provides 0.154 moles per liter, that is, contains 154 mEq / L of Na $^+$ and Cl $^-$. The fact contain more solute per liter,

---

[2] In chemistry, the normal concentration of sodium chloride is 0.5 mol of NaCl assuming complete dissociation. Physiological dissociation is approximately 1.7 ions per mole, so that a normal NaCl is 1/1.7 = 0.588 molar. This is approximately 4 times more concentrated than the medical term "normal saline" of 0.154 mol

makes this solution with a slightly higher osmolarity[3] than blood, on an average day the natremia[4] can range between 130-150 mEq / L (normonatremia) . However, the osmolarity of normal saline is very close to the osmolarity of the NaCl in the blood[22].

From Figure 22 and considering the dimensions of our saline cells, presents three values of resistivity, $\varrho = 2.65\Omega m$, $\varrho = 0.55\Omega m$ and $\varrho = 1.3\Omega m$, respectively.
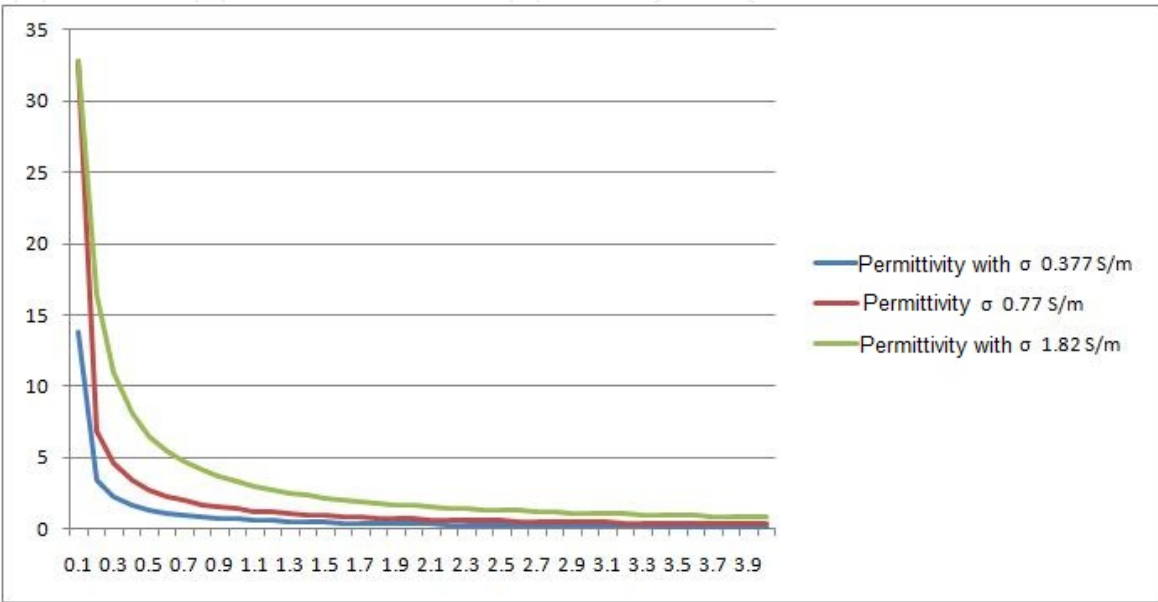

Figure 22. Measured frequency behavior of three electrolytic cells
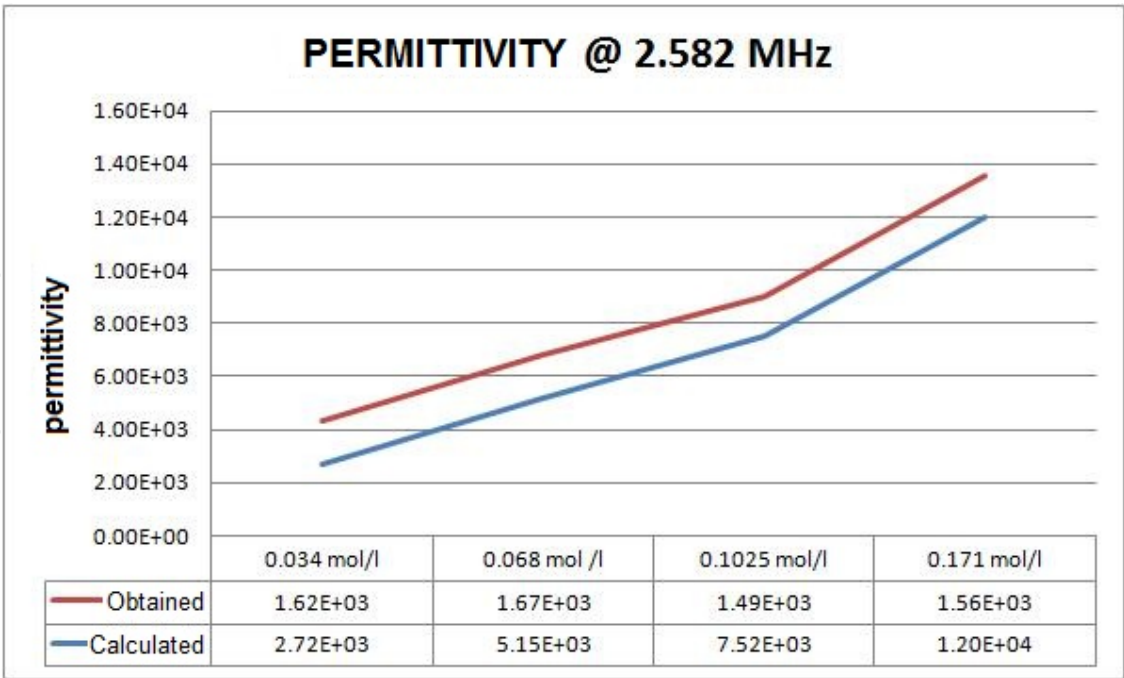
Figure 23. Saline solutions response at resonance frequency of the coil system

---

[3] Measuring solute concentration
[4] Concentration of sodium in the blood

Figure 23 presents a summary of values acquired with the network analyzer, Figure 24 represents the values obtained with the HP4192A impedance analyzer.
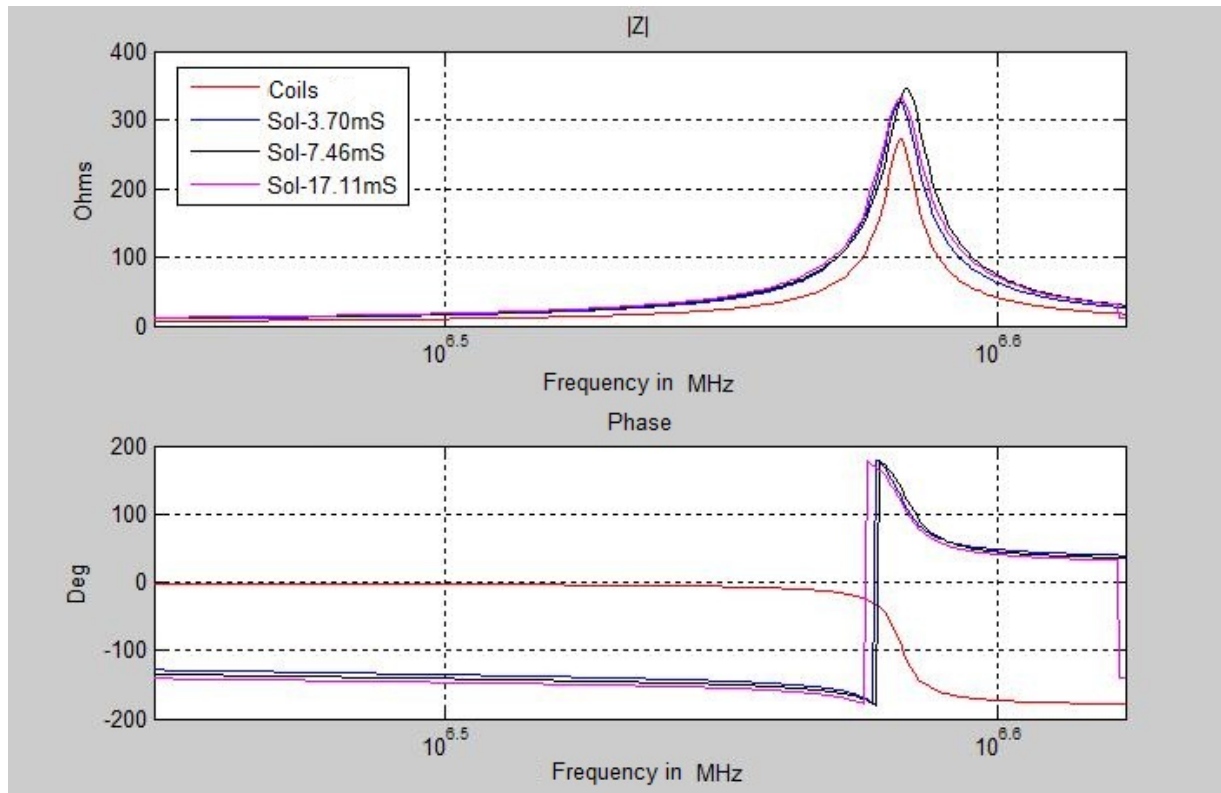
Figure 24. Frequency responses of Saline Solutions.

8. Biological suspensions

Typically, in vitro measures, is considered a sample of uniform section (A) and length (L), in the majority of cases it is more practical to consider the volume (V) in aqueous solutions. In this case the ratio between the conductivity and the permittivity of the sample with the resistance and reactance are:

$$C = \frac{\varepsilon \, \varepsilon_0 \, V}{L^2} \, [F] \tag{22}$$

$$R = \frac{L^2}{\sigma \, V} \, [\Omega] \tag{23}$$

$$Z = \frac{L^2}{(\sigma + j \, \omega \, \varepsilon \, \varepsilon_0) \, V} \tag{24}$$

Following experiments with saline solutions, was considered to have the information needed to proceed to carry out experiments with biological solutions, hence the first use of coil system as a reference and according to the above expressions, and also with a 500 mL volume, and a tank length of 85 mm was obtained with a suspension of high concentration of biomass (80 g / l of yeast), a 8.305 dB attenuation, comparing this with a 13.71 dB attenuation of coil system, this means a representation of a 65% increase in impedance in the suspension.

It should be mentioned that the embodiment of the vast majority of measurements for suspension was made with the HP4192A impedance analyzer, considering the structure and existing coil system, the utilization ratio of the impedance analyzer is because the probes used to interconnect arrangement coils are constructed on purpose, greatly decreasing the amount of error attributable to the length of the coaxial cables.
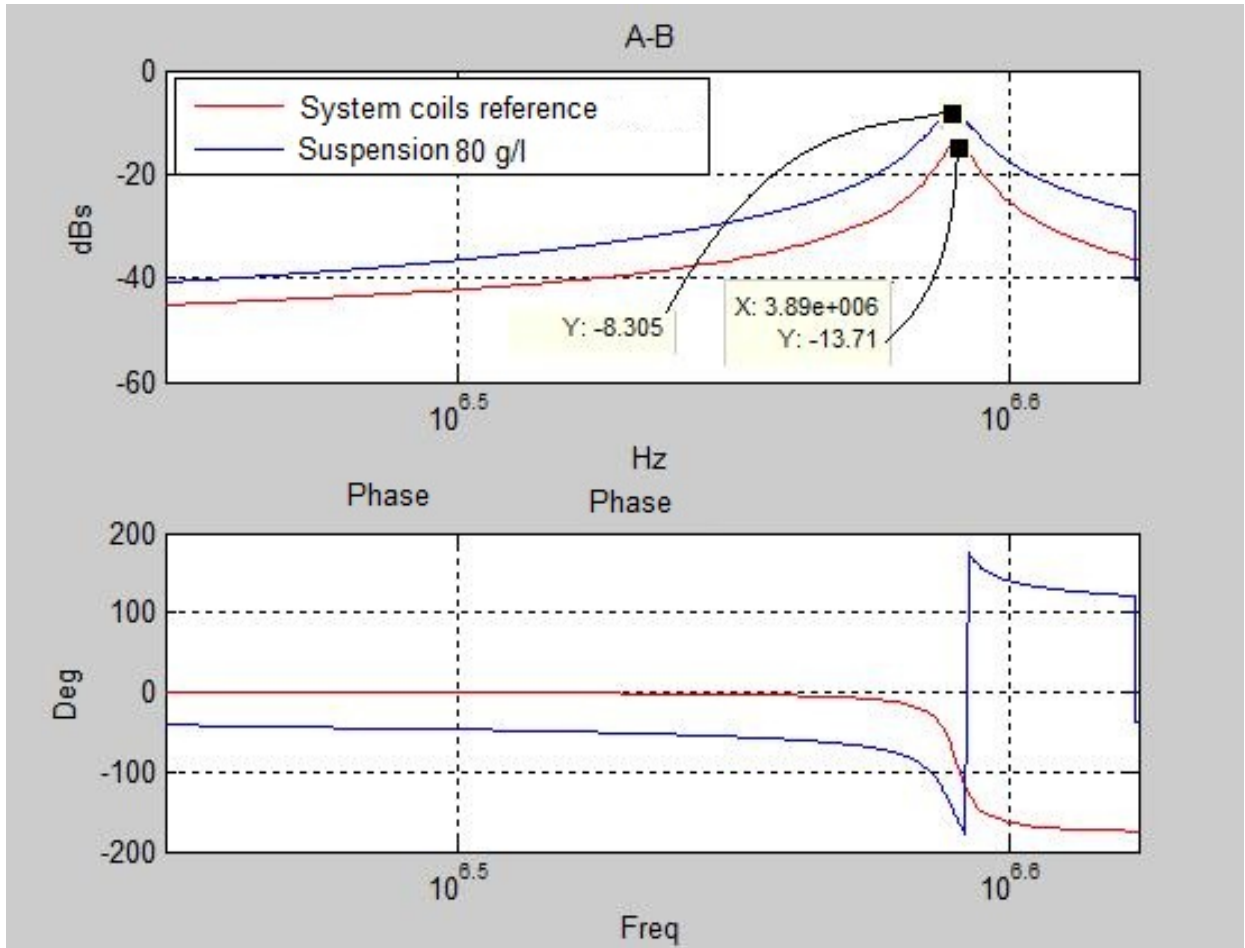
Figure 25. Impedance Representation of Biological Suspension, comparatively to the coil system.

After 35 minutes, the yeast was deposited at the bottom of the container; we proceeded to extract 350ml of water and recovered the same amount of water (350ml), but now with a salinity 8.78mS/cm.

The interesting thing in this experiment as shown in Figure 25, having increased conductivity, as a result of water replaced without electrolytes, with water with electrolytes (8.78mS/cm) decreased by 6% the impedance of the suspension by the lower proportion of yeast and major salinity, $Z_{lev} = 384.37\Omega$, $Z_{lev} + NaCl = 361.87\Omega$, $\Delta\Omega = 22.5$

9. Comparison of results

Measurements of saline cell and a biological suspension with HP impedance analyzer, allow us to characterize the results:

	Z (Ohms)	ε	μ (H/m)	σ (S/m)
2g NaCl	325.3	14.45	2.13E-04	0.00307409
4gNaCl	334.9	14.039	2.13E-04	0.00298597
10gNaCl	333.3	14.11	2.13E-04	0.0030003

Table 3. Characteristic values of a saline cell saline with varying degrees of salinity at resonance frequency of the coils system @ 3.825 MHz

	Z (Ohms)	ε	μ (H/m)	σ (S/m)
80g_yeast	395.64	11.68	2.16E-04	0.00252755
80g_yeast+6h	392.42	11.77	2.17E-04	0.00254829
80g_yeast+24h	385.08	11.99	2.17E-04	0.00259686

Table 4. Characteristic values of a biological suspension with various lengths of time at resonance frequency of the coils system @ 3.892 MHz

10. Conclusion

The presentation of results, by their very short nature, could be interpreted as an activity which is not time consuming, but the opposite is true, because from the moment of preparation of the experiments, there are always a number of imponderables, such as materials or materials that are needed to carry out the measurements do not have them, at least, operating conditions, climate, lighting, etc..

For the characterization of substances, suspensions and / or solutions must take into account, and in a very particular, maintain the same amounts, and make measurements in a repetitive manner, so as to place on record its findings to conditions geometric, physical and mechanical properties, different and contrast with conditions similar to those obtained. The measurements carried out with the Network Analyzer, which was mostly used equipment, are quite contrasting with measurements made with the HP impedance analyzer. As we can see with the first, which strongly influences the distance at which measurements were made, not with the impedance analyzer as it had a "fixture" on purpose.

Speaking of the actual material used and specific the experiment with saline cell, it was found that one of the factors that influence in the admittance at low frequencies is the electrical permittivity of water. The values depend on the frequency of measurements, and the frequency sweep, this due to the response of the dielectric constant of the solution, which varies considerably with frequency.

Using a saline solution with a high degree of salinity, more than 9 g / l of salt, we see that in the graphs of the results if $\varepsilon'' / \varepsilon' < 2$, the ε'' accuracy degrades. This may be because the impedance of solutions with high salt is essentially resistive. In an opposite manner with a "window" at 999 KHz frequency on average, before the resonance frequency of the coil circuit, the impedance of the solution is essentially reactive, and since this type of impedance measurements of reflection / transmission were performed mainly with the network analyzer is a significant higher level of uncertainty in measuring the smaller capacitive component where ε'' is derived.

The HP impedance analyzer measurements, both saline solutions and suspensions, allowed us to compare results, specifically ε'' values. In the suspensions could be evaluated especially an increase in the impedance, over time, possibly due to increased cell growth, hence an increase in the capacitive reactance of the suspension.

Considering the results obtained, we can consider the approach to the characterization as reasonably good since the relative permittivity is much greater than unity for the dielectric (both saline solutions and biological suspensions).

One of the properties of biological tissue, such as conductivity, is well reflected by the frequency dependence, particularly in the range of 10 KHz-10MHz (β dispersion range). The conductivity at low frequencies denotes the volume of extracellular fluid essence, the additional contribution of intracellular fluid volume with a significant increase in the applied frequency causes a significant increase in conductivity.

And finally and considering the substantial increase in interest in the development of magnetic induction spectroscopy (MIS) as a valid option for obtaining the conductivity of the human body without the need for direct contact with tissue (Korzhenevskii and Cherepenin 1997 Griffiths et al. 1999, Korjenevsky et al. 2000); In addition to other passive electrical properties of biological tissues (Hermann Scharfetter, Casañas Roberto and Javier Rosell, 2003).

Since MIS is based on measurements of small changes in magnetic fields, typically of the order of 1% or less at frequencies up to 10 MHz, and also because of their physical limitations is not recommended at frequencies below 10 kHz, this also represents a great challenge in electronic design, possibly one of its greatest disadvantages.

Author details

Jesús Rodarte Dávila, Jenaro C. Paz Gutierrez and Ricardo Perez Blanco
Department of Electrical and Computer Engineering, Juarez City Autonomous University,
North Charro Avenue, Juarez City, Chihuahua, México

Acknowledgement

11. References

[1] Grimnes S. Bioimpedance and Bioelectricity Basics, Academic Press ISBN 0-12-303260-1;p7

[2] Hoffer EC, Clifton KM, Simpson DC. Correlation of wholebody impedance with total body volume. J Appl Physiol 1969;27:531–4.

[3] Nyboer J. Electrical impedance plethysmograph, 2nd ed. Springfield, IL: CC Thomas; 1970.

[4] Boulier A, Fricker J, Thomasset A-L, Apfelbaum M. Fat-free mass estimation by the two-electrode impedance method. Am. J Clin. Nutr. 1990; 52:581–5.

[5] Harris A. Ductal epithelial cells cultured from human fetal epididymis and vas deferens: relevance to sterility in cystic fibrosis, Journal of Cell Science, Vol 92, Issue 4 687-690, Copyright © 1989 by Company of Biologists

[6] Asami K. Real-Time Monitoring of Yeast Cell Division by Dielectric Spectroscopy, Biophys J, June 1999, p. 3345-3348, Vol. 76, No. 6

[7] Ong K.G., Monitoring of bacteria growth using a wireless, remote query resonant-circuit sensor: application to environmental sensing. Copyright © 2001 Elsevier Science B.V. All rights reserved.

[8] Hofmann M. C., Transponder Based Sensor for Monitoring Electrical Properties of Biological Cell Solutions. Copyright © 2005 The Society for Biotechnology, Japan Published by Elsevier B.V.

[9] Scharfetter H., Casañas R., and Rosell J., "Biological Tissue Characterization by Magnetic Induction Spectroscopy (MIS): Requirements and Limitations,"IEEE Transactions on Biomedical Engineering, vol. 50, NO. 7, JULY 2003.

[10] http://www.ni.com/support/labview/lvtool.htm

[11] Service Manual R&S®ZVx Vector Network Analyzer Family: http://www2.rohde-schwarz.com/en/products/test_and_measurement/network_analysis/ZVx-%7C-Key_Facts-%7C-4-%7C-658.html

[12] Riedel C.H., Keppelen M., Nani S., Merges R.D. y Dössel. (2004) "Planar System for Magnetic Induction Conductivity Measurement Using a Sensor Matrix". Institute of Physics Publishing., Physiol. Meas. 25

[13] Rodarte J. (2008) Método Experimental de Medida de Impedancias Inalámbricamente Usando un Analizador de Redes. Instituto Tecnológico De Chihuahua., Electro 2008.

[14] Ong, K.G. and Grimes, C. A., "A resonant printed-circuit sensor for remote query monitoring of environmental parameters". Smart Mater. Struct., 9, 421–428 (2000).

[15] Edminister J., Nahvi M., "CIRCUITOS ELECTRICOS Y ELECTRONICOS", Cap. 13. Cuadripolos (circuitos de dos puertas), ISBN: 8448145437, Ed: McGrawHill, Serie Schaum

[16] Calculation of Formulae - Self-inductance ; www.ivorcatt.com/6_2.htm

[17] Donaldson N.deN., Perkins T.A., "Analysis of resonant coupled coils in the design of radio frequency transcutaneous links" , Med. & Biol. Eng. & Comput., 1983, 21, 612-627

[18] Commercial Software "PSpice" Ver 9.2 Copyright 1886-1999 by Cadence Design Systems

[19] Kenneth W. Misevich, Capacitive Humidity Transducer, IEEE Transactions on Industrial Electronics and Control Instrumentation, vol. IECI-16, NO. 1, JULY 1969.

[20] Mathcad, version 14.0.0.163 Copyright © 2007 Parametric Technology Corporation. All Rights Reserved.

[21] Pething, 1979 R. Pething. Dielectric and Electronic Properties of Biological Materials, Wiley (1979).

[22] Awad S., Allison S.P., Lobo D.N., "The history of 0.9% saline.", Clin. Nutr. 2008 Apr; 27 (2): 179-88. Epub 2008 Mar 3.